Progress In Electromagnetics Research M, Vol. 3, 177–191, 2008

VELOCITY SHEAR ION-CYCLOTRON INSTABILITY WITH PERPENDICULAR AC ELECTRIC FIELD

R. S. Pandey and U. C. Srivastava

Department of Applied Physics
Amity School of Engineering
Amity University
Noida UP, India

R. P. Pandey, B. B. Prasad, and Hariom

Department of Physics
Veer Kunwar Singh University
Ara (Bihar), India

Abstract—Current driven electrostatic ion cyclotron instability has been studied for parallel flow velocity shear with perpendicular a.c. electric field to the ambient magnetic field for bi-Maxwellian density drift distribution function. The method adopted for expression for dispersion relation and growth rate is kinetic approach and method of characteristic solution for ionospheric plasma. The effect of a.c. frequency, density gradient, and velocity shear scale length has been discussed.

1. INTRODUCTION

The plasma has been assumed to be essentially infinite and homogeneous in accordance with the model originally proposed by [1]. A series of papers [2–5] have given a detailed account of non-local EICI theories. They have studied the influence of magnetic shear as well as that of a finite width of the current channel. The dynamics that govern the release of free energy associated with sheared flows have been a matter of interest both in hydrodynamics [6] and in plasma physics [7]. This release of free energy is accompanied almost invariably by the onset of instabilities, which in turn, play an important role in a variety of physical processes. For example, in hydrodynamic systems, shear-driven instabilities can cause a transition from laminar to turbulent flow [8] while in fusion plasma, sheared flows have been found to modify significantly the magneto-hydrodynamic equilibrium and ballooning stability of toroidal confinement devices [8, 9]. More importantly, shear-driven turbulence can have a significant effect on particle, momentum and energy transport. Velocity shear, for instance, has been recently identified as an important element in the transition from L to H-mode confinement in tokamak plasmas [10–13]. Due to parametric constraints, however, in fusion studies, assumption is made for shear driven phenomena that the shear scale length is much larger than the ion Larmor radius. Although this assumption is in conformity with the experimental observations, it fixes the time scale of variation of the radiant shear-driven phenomena to be much larger than the ion gyro period (provided that the maximum drift speed is not much larger than the electron thermal speed).

Electrostatic ion-cyclotron waves are of interest due to the collissionless ion damping inherent to these types of waves. Consequently, their production in plasma could be an important means of heating ions in many plasma devices such as tokamaks and multiples. Recently, several papers have discussed the excitation of electrostatic ion-cyclotron waves by parametric instabilities. Electrostatic ion-cyclotron waves can act as a means of transferring the energy of a magneto-sonic wave to the ions of a plasma, it would be useful to understand the manner in which density, temperature and magnetic field gradients as well as shear, alter the dispersion of the waves and their excitation by parametric processes. This is especially true in view of the significant effect which density gradients have seen on parametric instabilities when $\omega \approx \omega_{pe}$ (where ω_{pe} is the electron plasma frequency).

Considering the specific case of electrostatic ion cyclotron waves in the presence of density gradient and a uniform magnetic field, the energy loss across the gradient and so the damping of the wave can be expected to be minimized if the primary propagation is in the y direction (i.e., $k_y \gg |k_z|$). Next, it is assumed that the gyro-radius ρ_s are much smaller than the density gradient scale length L_n as well as the scale length of the waves in the absence of a pump magneto-sonic wave.

The presence of gradients in plasma can localize parametric instabilities in space in three different ways. First there is the possibility that gradients can change the wave number in the direction of the inhomogeneity and thereby create a mismatch in the wave significant for the case of the decay instability with $\omega \approx \omega_p$. A second possibility which may occur is to have coupling coefficients or functions of position. This is particularly important for the purely growing mode and in the convective or absolute nature of the decay instability in bounded plasma. Generation of ion-cyclotron like wave by parallel flow velocity shear in the presence of inhomogeneous D.C. electric field in an anisotropic magnetoplasma has been studied by [14]. Density and magnetic field gradients can influence the dispersion of electrostatic ion-cyclotron waves and their excitation by the cyclotron decay instability. Temperature gradients are not so significant since electrostatic ion-cyclotron waves are much more sensitive to magnetic field variations.

Density gradients affect the threshold of the cyclotron decay instability due to wave energy transport across the gradient and the resultant enhancement of the damping for one of the excited waves while magnetic field gradients introduce a mismatch in wave number, which if large enough, can increase the threshold.

The motivation for this work is provided by observations of both space and laboratory plasmas in which flows have been reported, whose shear scale length can be of the order of the ion Larmor radius or smaller. In auroral phenomena; for example, electric fields called paired electrostatic shocks have been found to exist whose scale length of variation is of the order of the ion Larmor radius [15, 16]. These electric fields cause localized cross-field flows, which excite instability with frequency and growth rate in the vicinity of the ion cyclotron frequency [17, 18]. A distinctive feature of this instability is that it can exist even when the field-aligned current is sub-critical. Another example of a strongly sheared system is given by the dynamical evolution of the plasma sheet just prior to the on set of a magnetic sub storm. During this time, the neutral plasma sheet region becomes thin and its width becomes smaller than the ion Larmor radius.

In this paper, electrostatic ion-cyclotron parallel flow velocity shear instability has been studied in the presence of perpendicular AC electric field. The method of characteristic solution has been used for the study. The effect of AC electric field, density gradient and velocity shear length has been studied in the region of ionosphere for long wavelength.

2. DISPERSION RELATION

A spatially homogeneous an-isotropic collision less plasma subjected to an external magnetic field $B_0 = B_0 e'z$ and an electric fields $E_{0x} = (E_0 \sin \upsilon t e' x)$ has been considered. In order to obtain the dispersion relation in this case, the Vlasov-Maxwell equations are linearized. The linearized equations obtained after neglecting the higher order terms and separating the equilibrium and non equilibrium parts, following the techniques of [19, 20], are given as

$$v\frac{\delta f_{s0}}{\delta r}+\frac{e_s}{m_s}\left[E_o\sin\,\upsilon\,t+(v\times B_o)\right]\left(\frac{\delta f_{so}}{\delta v}\right)=0 \tag{1}$$

$$\frac{\delta f_{s1}}{\delta t}+v\frac{\delta f_{s1}}{\delta r}+\left(\frac{F}{m_s}\right)\left(\frac{\delta f_{s1}}{\delta v}\right)=S(r,v,t) \tag{2}$$

where force is defined as $F = mdv/dt$

$$F=e_s\left[E_0\;Sin\;\upsilon t+(v\times B_0)\right] \tag{3}$$

The practical trajectories are obtained by solving the equation of motion defined in Equation (3) and $S(r, v, t)$ is defined as

$$S(r,v,t)=\frac{-e_s}{m_s}\left[E_1+(v\times B_1)\right]\left(\frac{\delta\;f_{so}}{\delta v}\right) \tag{4}$$

where s denotes species and E_1, B_1 and f_{s1} are perturbed and are assumed to have harmonic dependence in f_{s1}, B_1 and $E_1 \sim \exp i(k.r - \omega t)$. The method of characteristic solution is used to determine the perturbed distribution function. f_{s1}, which is obtained from Equation (2) by

$$f_{s1}(r,v,t)=\int_{\circ 0^\circ}^{\infty}S\left\{r_o\left(r,v,t'\right),v_0\left(r,v,t'\right),t-t'\right\}dt' \tag{5}$$

The phase space coordinate system has been transformed from (r, v, t) to $(r_0,\ v_0,\ t - t')$. The particle trajectories which have been obtained by solving Equation (3) for the given external field configuration and wave propagation

$$k=\left[k_\perp e_x,0,k_\parallel e_z\right].$$

are

$$\begin{aligned}X_0&=X+\left(\frac{v_y}{\Omega_{cs}}\right)+\left(\frac{1}{\Omega_{cs}}\right)\left[v_x\cos\Omega_{cs}t'-v_y\cos\Omega_{cs}t'\right]\\&\quad+\left(\frac{\Gamma_x}{\Omega_{cs}}\right)\left[\frac{\Omega_{cs}\sin\upsilon t'-\upsilon\sin\Omega_{cs}t'}{\Omega_{cs}^2-\upsilon^2}\right]\\Y_0&=y+\left(\frac{v_x}{\Omega_{cs}}\right)-\left(\frac{1}{\Omega_{cs}}\right)\left[v_x\cos\Omega_{cs}t'-v_y\sin\Omega_{cs}t'\right]\\&\quad-\left(\frac{\Gamma_x}{\upsilon\omega_{cs}}\right)\left[\frac{\upsilon^2\cos\Omega_{cs}t'-\Omega_{cs}^2\cos\upsilon\,t'}{\Omega_{cs}^2-\upsilon^2}\right]\\Z_0&=Z-v_zt'\end{aligned} \tag{6}$$

and the velocities are

$$\begin{aligned} v_{x0} &= v_x \cos\Omega_{cs}t' - v_y \sin\Omega_{cs}t' + \left\{ \frac{\nu\Gamma_x(\cos\upsilon t' - \cos\Omega_{cs}t')}{\Omega_{cs}^2 - \upsilon^2} \right\} \\ v_{y0} &= v_x \sin\Omega_{cs}t' + v_y \cos\Omega_{cs}t' - \left\{ \frac{\Gamma_x(\Omega_{cs}\sin\upsilon\, t' - \upsilon\sin\Omega_{cs}t')}{\Omega_{cs}^2 - \upsilon^2} \right\} \\ v_{z0} &= v_z \end{aligned} \tag{7}$$

where υ=a.c.frequency, $\Omega_{cs} = \frac{e_s B_0}{m_s}$ is the cyclotron frequency of species "s" and $\Gamma_x = \frac{e_s E_0}{m_s}$. Equation (2) can be written in terms of a perturbed quantities as

$$\begin{aligned} S\left(r_o, v_o, t-t'\right) \;=\; & -\left(\frac{e_s}{m_s\Omega}\right) e^{i\{kr_0(r,v,t)-\Omega(t-t')\}} \\ & + \left[(\Omega - k.v_o)\, E_1 + (v_0.E_1)\, k\right] \left(\frac{\delta f_{s0}}{\delta v}\right) \end{aligned} \tag{8}$$

The unperturbed distribution function with velocity and density gradient is given by [20, 21].

$$\begin{aligned} f_{so} &= f_{mo} + v_y \varepsilon'' \\ \varepsilon'' &= \frac{1}{\Omega_s}\left[\varepsilon_n + \frac{2(v_\parallel - v_{oz}(x))}{\alpha_{\parallel s}^2} \frac{dv_{oz}(x)}{dx}\right] \\ f_{mo} &= \frac{n_0(x)}{\pi^{3/2}\alpha_\perp^2 \alpha_\parallel} \exp\left[-\frac{v_{ox}^2 + v_{oy}^2}{\alpha_{\perp s}^2} - \frac{(v_\parallel - v_{oz}(x))^2}{\alpha_{\parallel s}^2}\right] \end{aligned} \tag{9}$$

where ε'' being constant of motion

$$\alpha_{\perp,\parallel s}^2 = \left(\frac{2K_B T_\perp T_{\parallel s}}{m_s}\right) \tag{10}$$

After using the unperturbed trajectories with perpendicular AC electric field and unperturbed distribution function, also doing some lengthy simplifications the perturbed distribution function has been found as

$$\begin{aligned} f_{s1}(r,v,t) = & -\frac{ie_s}{m_s\omega} \sum_{m,n,p,q}^{\infty} \frac{J_p(\lambda_2) J_n(\lambda_1) J_m(\lambda_1) J_g(\lambda_3)}{\{\omega - k_\parallel v_\parallel - (n+g)\omega_{cs} + p\upsilon\}} \\ & \times \left[E_{1x}U^* + E_{1y}V^* + E_{1z}W^*\right] e^{(m-n)(\pi/2+\theta)} e^{i(g-p)(\pi/2+\theta)} \end{aligned} \tag{11}$$

$$
\begin{aligned}
U^* &= C_1\left(v_\perp \frac{n}{\lambda} + \frac{\upsilon\Gamma_x}{\omega_{cs}^2 - \upsilon^2}\left(\frac{p}{\lambda_2} - \frac{n}{\lambda_1}\right)\right)\\
C_1 &= (\omega - k_\parallel \cdot v_\parallel)\left(\frac{-2f_{so}}{\alpha_{\perp s}^2}\right) + k_\parallel\left(\frac{\partial f_{s0}}{\partial v_\parallel}\right)\\
V^* &= iC_1\left[v_\perp \frac{J'_n}{J_n} + \frac{\Gamma_x}{\omega_{cs}^2 - \upsilon^2}\left\{\Omega_c \frac{J'_p}{J_p} - \upsilon \frac{n}{\lambda_1}\right\}\right]\\
&\quad + \varepsilon''\left(1 - k_\perp v_\perp \frac{n}{\lambda_1} - k_\perp \frac{\upsilon\Gamma_x}{\omega_{cs}^2 - \upsilon^2}\left\{\frac{p}{\lambda_2} - \frac{n}{\lambda_1}\right\}\right)\\
W^* &= Dv_\perp k_\perp \frac{n}{\lambda_1} + \omega \frac{\partial f_{s0}}{\partial v_\parallel} + D\frac{k_\perp \upsilon\Gamma_x}{\omega_{cs}^2 - \upsilon^2}\left(\frac{p}{\lambda_2} - \frac{n}{\lambda_1}\right)\\
D &= v_\parallel\left(\frac{-2f_{so}}{\alpha_{\perp s}^2}\right) - \left(\frac{\partial f_{s0}}{\partial v_\parallel}\right)\\
\lambda_1 &= \frac{k_\perp v_\perp}{\omega_{cs}}, \quad \lambda_2 = \frac{k_\perp \Gamma_x \upsilon}{\omega_{cs}^2 - \upsilon^2}, \quad \lambda_3 = \frac{k_\perp \Gamma_x \omega_{cs}}{\omega_{cs}^2 - \upsilon^2}\\
J'_n &= \frac{dJ_n(\lambda_1)}{d\lambda_1}, \quad J'_p = \frac{dJ_p(\lambda_2)}{d\lambda_2}
\end{aligned}
\tag{12}
$$

Now simplifying $m = n,\ g = p$ and using the definition of current density, conductivity and dielectric tensor, we get the dielectric tensor as

$$
\varepsilon_{ij}(k,\omega) = 1 - \sum_s \frac{4\pi\pi_s^2}{m_s\omega^2}\int \sum_{np} \frac{J_p(\lambda_2)J_q(\lambda_3)d^3v\,\|s_{ij}\|}{\omega - k_\parallel v_\parallel - (n+q)\omega_{cs} + p\upsilon}
\tag{13}
$$

where

$$
\|s_{ij}\| = \left\| \begin{matrix} v_\perp J_n^2 U^* \frac{n}{\lambda_1} & v_\perp J_n^2 V^* \frac{n}{\lambda_1} & v_\perp J_n^2 \frac{n}{\lambda_1} W^* \\ -iv_\perp J'_n J_n U^* & -iv_\perp J'_n J_n V^* & -iv_\perp J'_n J_n W^* \\ v_\parallel J_n^2 U^* & v_\parallel J_n^2 V^* & v_\parallel J_n^2 W^* \end{matrix} \right\|
\tag{14}
$$

Now, we consider electrostatic Ion cyclotron instability;

$$
\|\varepsilon_{ii}\| = N^2
\tag{15}
$$

where $N =$ refractive index.

The required electrostatic dispersion relation can be obtained by using the technique of [14, 19] and from Equation (1) to (15)

$$\begin{aligned} D(k,\omega) \;=\; & 1+\frac{2\omega_{ps}^2}{k_\perp^2\alpha_{\perp s}^2}\Gamma_n(\mu_s)\sum J_p(\lambda_2)J_g(\lambda_3)\eta_s\frac{k_\perp}{k_\parallel} \\ & \times\left[\left\{\frac{\bar{\omega}}{k_\parallel\alpha_{\parallel s}}-\frac{1}{2}\varepsilon_n\rho_s\frac{\alpha_{\perp s}}{\alpha_{\parallel s}}\right\}Z(\xi_s)-A_s\frac{\alpha_{\perp s}^2}{\alpha_{\parallel s}^2}\left(1+\xi_s Z(\xi_s)\right)\right. \\ & \left.+A_T\frac{k_\parallel}{k_\perp}\left(1+\xi_s Z(\xi_s)\right)\right] \end{aligned} \tag{16}$$

where $Z(\xi)$ is plasma dispersion function,

$$\begin{aligned} \xi &= \frac{\varpi-(n+g)\Omega_s+\upsilon p}{k_\parallel\,\alpha_{\parallel s}}, \\ \eta_s &= \left[1-\frac{\upsilon\Gamma_{xs}}{\alpha_{\perp s}(\Omega_s^2-\upsilon^2)}+\frac{\upsilon p}{n\Omega_s}\right], \\ A_s &= \frac{1}{\Omega_s}\frac{dv_{oz}(x)}{dx},\quad A_T=\frac{\alpha_\perp^2}{\alpha_{\parallel s}^2}-1,\quad \varepsilon_n=\frac{\delta l_n n(x)}{\delta x}, \\ \bar{\omega} &= \omega-k_\parallel v_{oz}(x),\quad \mu_s=\frac{k_\perp^2\rho_s^2}{2},\quad \lambda_{Ds}^2=\frac{\alpha_{\perp s}^2}{2\omega_p^2}, \\ \omega_p^2 &= \text{Plasma frequency} \\ \Gamma_n(\mu_s) &= \text{Modified Bessel Function} \end{aligned} \tag{17}$$

Now above dispersion relation Equation (16) reduces to that of [21] if inhomogeneous AC electric field is set to zero, $\alpha_\perp = \alpha_{\parallel s}$ and n equals to zero. If AC field is removed and inhomogeneous DC electric field is introduced with the condition $n \neq$ zero the above dispersion relation Equation (16) reduces to that of [14].

Following [19, 21] for $p = 1$, $g = 0$ and $s = ie$, we get dispersion relation for electrons and ions. For electrons, $k_\perp\rho_e \ll 1$ and for ions no such assumption is made. Thus above equation becomes:

$$\begin{aligned} D(k,\omega) \;=\; & 1+\frac{1}{k_\perp^2\lambda_{De}^2}\eta_e\frac{T_{\perp e}}{T_{\parallel e}}+\frac{1}{k_\perp^2\lambda_{Di}^2}\eta_i\left\{\frac{T_{\perp i}}{T_{\parallel i}}\Gamma_n(\mu_i)\frac{k_\perp}{k_\parallel}\right. \\ & \left\{\left(\frac{\bar{\omega}}{k_\parallel\alpha_{\parallel i}}\frac{T_{\perp i}}{T_{\parallel i}}-\frac{1}{2}\varepsilon_n\rho_i\frac{\alpha_{\perp i}}{\alpha_{\parallel i}}-\frac{n\Omega_i+p\upsilon}{k_\parallel\alpha_{\parallel i}}A_T\right)Z(\xi_i)\right. \\ & \left.\left.-A_i\frac{T_{\perp i}}{T_{\parallel i}}\left(1+\xi_i Z(\xi_i)\right)\right\}\right\}, \end{aligned}$$

After substituting $Z(\xi_i) = -(1/\xi_i) - (1/2\xi_i^3)$, $n_{0i} = n_{0e}$ and multiplying throughout by $k_\perp^2\lambda_{Di}^2/\eta_i$,

$$\begin{aligned} 0 \;=\; & \frac{\lambda_{Di}^2\eta_e T_{\perp e}}{\lambda_{De}^2\eta_i T_{\parallel e}} + \left\{\frac{T_{\perp i}}{T_{\parallel i}} - \Gamma_n(\mu_i)\frac{T_{\perp i}}{T_{\parallel i}} + \frac{\Gamma_n(\mu_i)k_\perp\varepsilon_n\rho_i\alpha_{\perp i}}{2k_\parallel\alpha_{\parallel i}}\right. \\ & \times\frac{k_\parallel\alpha_{\parallel i}}{\varpi - n\Omega_i + p\nu} - \frac{\Gamma_n(\mu_i)k_\perp}{k_\parallel} \times \frac{k_\parallel\alpha_{\parallel i} + n\Omega_i}{\varpi - n\Omega_i + p\nu} \\ & \left. - \frac{\Gamma_n(\mu_i)}{2\left(\varpi - n\Omega_i + p\nu\right)^2} \times \frac{T_{\perp i}}{T_{\parallel i}}(k_\parallel\alpha_{\parallel i})^2\left(1 - \frac{k_\perp}{k_\parallel}A_i\right)\right\}, \end{aligned} \tag{18}$$

where

$$\begin{aligned} \eta_e &= \left[1 - \frac{\upsilon\Gamma_{xe}}{\alpha_{\perp e}(\Omega_e^2 - \upsilon^2)} + \frac{\upsilon p}{n\Omega_e}\right], \\ \eta_i &= \left[1 - \frac{\upsilon\Gamma_{xi}}{\alpha_{\perp i}(\Omega_i^2 - \upsilon^2)} + \frac{\upsilon p}{n\Omega_i}\right], \end{aligned} \tag{19}$$

Multiplying throughout in Equation (18) by $\left(\frac{\varpi - n\Omega_i + p\upsilon}{k_\parallel\alpha_{\parallel i}}\right)^2$, we obtain a quadratic dispersion as:

$$a_1\left(\frac{\bar{\omega}'}{\Omega_i}\right)^2 + b_1\left(\frac{\bar{\omega}'}{\Omega_i}\right) + c_1 = 0, \tag{20}$$

where

$$\begin{aligned} a_1 \;&=\; a_2\left(\frac{\Omega_i}{k_\parallel\alpha_{\parallel i}}\right)^2, \quad a_2 = \frac{T_{\perp i}}{T_{\parallel e}}\frac{\eta_e}{\eta_i} + \frac{T_{\perp i}}{T_{\parallel i}} - \Gamma_n(\mu_i)\frac{T_{\perp i}}{T_{\parallel i}}, \\ b_1 \;&=\; \frac{\Omega_i}{k_\parallel\alpha_{\parallel i}}b_2 - \frac{2p\upsilon}{\left(k_\parallel\alpha_{\parallel i}\right)^2}a_2\Omega_i, \\ b_2 \;&=\; \frac{k_\perp\Gamma_n(\mu_i)\varepsilon_n\rho_i\alpha_{\perp i}}{2k_\parallel\alpha_{\parallel i}} - \frac{k_\perp\Gamma_n(\mu_i)}{k_\parallel} - \frac{k_\perp\Gamma_n(\mu_i)n\Omega_i}{k_\parallel^2\alpha_{\parallel i}}, \\ c_1 \;&=\; \frac{\Gamma_n(\mu_i)T_{\perp i}}{2T_{\parallel i}}\left(1 - \frac{k_\perp}{k_\parallel} + A_i\right) - \frac{b_2 p\upsilon}{k_\parallel\alpha_{\parallel i}} + \frac{k_\perp^2\upsilon^2p^2}{\left(k_\parallel\alpha_{\parallel i}\right)^2}a_2, \end{aligned}$$

The solution of Equation (20) is

$$\bar{\omega}' = \frac{-b_1}{2a_1}\left[1 \pm \left(1 - \frac{4a_1c_1}{b_1^2}\right)^{1/2}\right] \tag{21}$$

From this expression, dimensionless growth rate has been calculated by computer technique when $b_1^2 = 4a_1c_1$. Hence, this criteria gives a condition for the growth rate of wave when

$$A_i > \frac{k_\parallel}{k_\perp}\left\{1 - \frac{2T_{\parallel i}}{\Gamma_n(\mu_i)T_{\perp i}}\left[\frac{\left(\frac{b_2\Omega_i}{k_\parallel\alpha_{\parallel i}} - \frac{2k_\perp p\upsilon}{\left(k_\parallel\alpha_{\parallel i}\right)^2}\right)^2}{4a_2\left(\frac{\Omega_i}{k_\parallel\alpha_{\parallel i}}\right)^2} + \frac{b_2p\upsilon}{k_\parallel\alpha_{\parallel i}} - \frac{\upsilon^2p^2}{\left(k_\parallel\alpha_{\parallel i}\right)^2}a_2\right]\right\} \tag{22}$$

If the contribution of AC electric field is removed $\alpha_{\parallel s}$ is made equal to $\alpha_{\perp s}$ and n equals to zero, Equation (18) reduces to that of [21] and in the absence of AC electric field and in the presence of DC electric field and $n \neq$ zero, growth rate expression given by Equation (18) reduces to that of [14].

3. RESULT AND DISCUSSION

Following plasma parameters taken from [14, 21] suited to the ionospheric region, have been used to evaluated the growth rate. Magnetic field B_0 has been taken to vary from $4\times10^{-7}\,T$ to $6\times10^{-7}\,T$, energy of the electrons $K_BT_\parallel = 10\,\text{eV}$, velocity shear scale length A_i has been allowed to vary between 0.5 to 0.55 and temperature gradient scale length $\varepsilon_n\rho_i$ between 0.02 to 0.05 and temperature ratio T_e/T_i between 2 to 4. The value of AC electric field has been fixed on $E_0 = 4\times10^{-3}\,\text{V/m}$ where as it frequency υ is allowed to vary between 2 KHz and KHz. Temperature anisotropy varies between 0.25 and 0.5 the value of θ varies from 88° to 88.5° where as $\theta = \tan^{-1}\left(\frac{k_\perp}{k_\parallel}\right)$.

Growth rate variations with $k_\perp\rho_i$ have been calculated from expression (18) for first and second harmonics $n = 1$, for various values of above given plasma parameters. Figure 1 exhibits the variation of growth rate with respect to $k_\perp\rho_i$ for two shear scale lengths at different harmonics. It is obvious from the figure that the growth rate increases by increasing the velocity shear scale length and maxima shifts towards higher values of $k_\perp\rho_i$. Growth rate increases with increase of harmonics. If the present results are compared with that obtained by [14] in which instead of A.C. electric field, they have studied the effect of inhomogeneous D.C. electric field and have performed calculations for the growth rate for the same plasma-parameters. It is found that while in the presence of D.C. electric

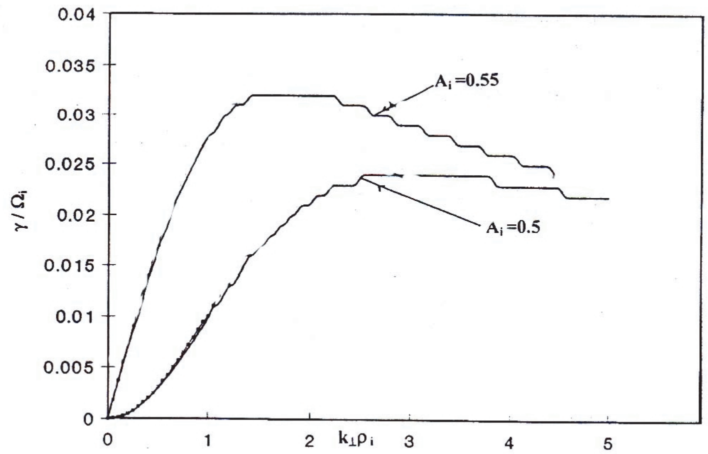

Figure 1. Variation of growth rate with $k_\perp \rho_i$ for various values of velocity shear scale length at other fixed plasma parameters.

field, the growth rate decreases and the instability is excited for value $k_\perp \rho_i > 1$ in short wave length region, the presence of AC electric field increases the growth rate and instability is excited for $k_\perp \rho_i > 1$ for a wide range of wave length region. The mechanism for instability of this mode is due to coupling of regions of positive and negative wave energy. This coupling occurs if velocity shear is non-uniform and the shear is the source of energy. Figure 2 deals with variation of growth rate with $k_\perp \rho_i$ for different values of θ. The growth rate increases by increasing the values of theta for 88° to 88.5° and maxima shifts towards lower value of $k_\perp \rho_i$ for both harmonics. In Figure 3, it is shown that change in magnetic field affects the growth rate. It increases by increasing the value of B_0 and maxima slightly shifts for lower values of $k_\perp \rho_i$. In homogeneity in magnetic field introduces a shear in velocity flow and couples positive and negative energy waves leading to growth of the wave. In Figure 4, the growth rate is affected by the ratio T_e/T_i. It is increased by increasing the value of T_e/T_i and maxima shifts towards higher values of $k_\perp \rho_i$ as the velocity shear term is proportional to T_e/T_i. In all the cases growth rate is less for higher harmonics. When shear flow is dominated by electron flows, the maxima flows towards lower wave lengths as in the case when $T_e/T_i = 3$. As it is clear from Figure 5 the growth rate increases by increasing the value of temperature anisotropy, growth rate is higher for higher harmonics and maxima coincides without any shift. The non-isothermal plasma changes the velocity shear required for onset of this instability.

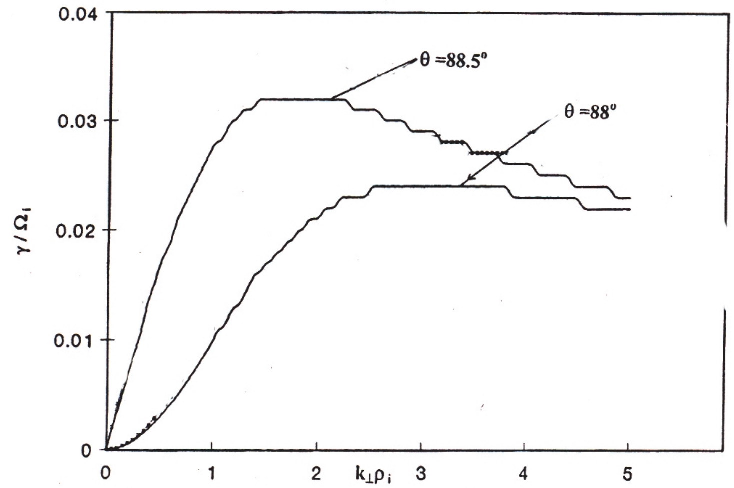

Figure 2. Variation of growth rate with $k_\perp \rho_i$ for various values of $\theta = \tan^{-1}\left(\frac{k_\perp}{k_\parallel}\right)$ at other fixed plasma parameters.

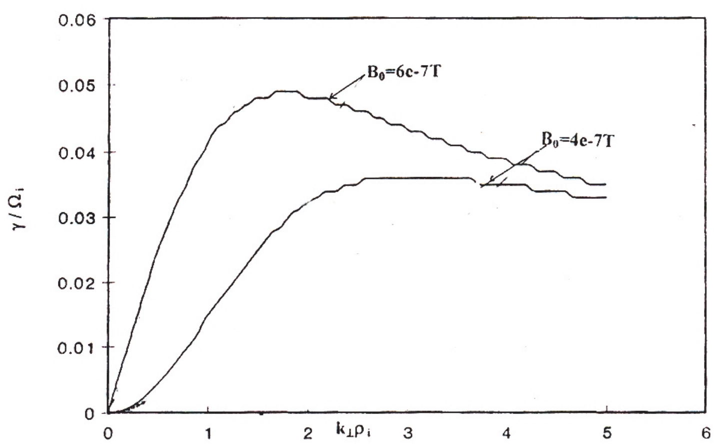

Figure 3. Variation of growth rate with $k_\perp \rho_i$ for various values of magnetic field B_0 at other fixed plasma Parameters.

In Figure 6, the effect of temperature gradient on growth rate has been shown. The growth rate increases by increasing the value of temperature gradient scale length with no change of the maxima. For $\varepsilon_n \rho_i = 0.02$, there is no change in the growth rate. But with the

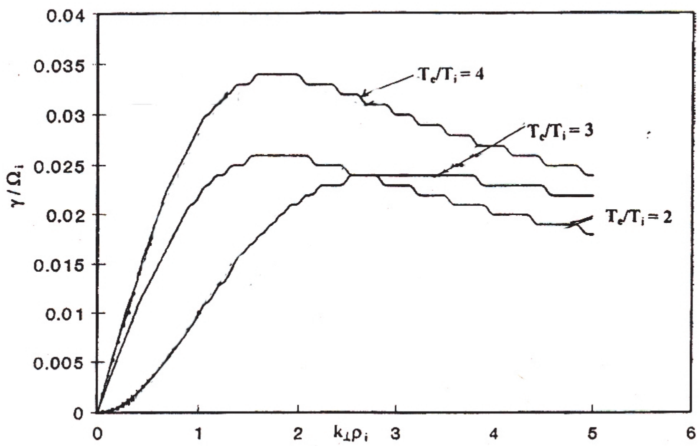

Figure 4. Variation of growth rate with $k_\perp \rho_i$ for various values of temperature ratio T_e/T_i other fixed plasma parameters.

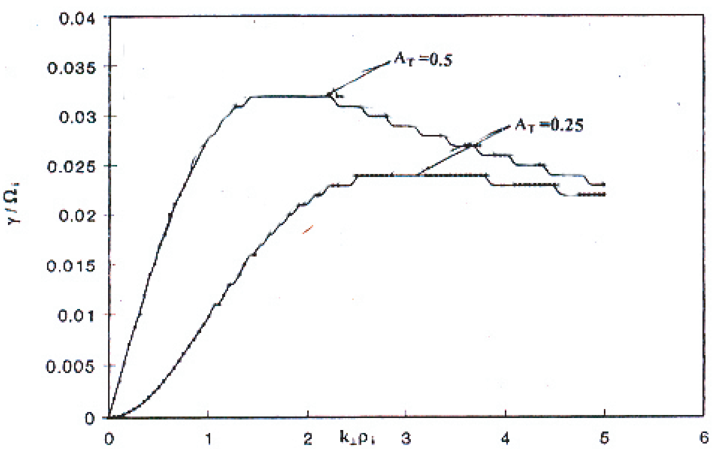

Figure 5. Variation of growth rate with $k_\perp \rho_i$ for various values of temperature anisotropy A_T at other fixed plasma parameters.

increase of the temperature gradient scale length, growth rate is higher. The temperature gradient has weak stabilizing effect on shear-driven K-H instability. If the temperature gradient is weaker than electron density gradient, then it is having stabilizing effect. However, the large temperature gradient in perpendicular direction increases the growth rate. It shows the stabilizing nature in K-H instability for $\beta > 1$. Figure 7 shows the variation of growth rate with respect to $k_\perp \rho_i$ for

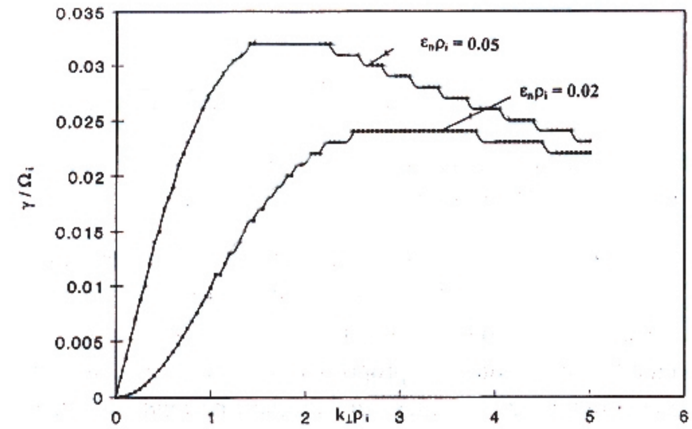

Figure 6. Variation of growth rate with $k_\perp \rho_i$ for various values of density gradient scale length at other fixed plasma parameters.

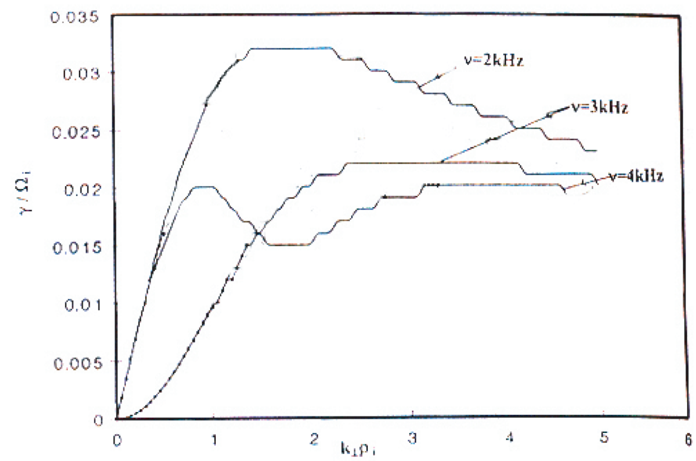

Figure 7. Variation of growth rate with $k_\perp \rho_i$ for various values of frequency of AC field at other fixed plasma parameters.

various values of AC field frequency. It is obvious from the figure that the growth rate decreases with the increase of AC field frequency with the shift of the maxima towards higher values of $k_\perp \rho_i$. For lower values of AC field frequency, the instability is excited in a localized region below $k_\perp \rho_i < 2$, but for higher AC field frequency the maxima shifts towards higher values of $k_\perp \rho_i$ and excitation of instability does not remain localized. Values of AC field frequency remain effective for a wide range of wavelength region for excitation of instability.

This effect would be of importance when electromagnetic effects are included. In general, this has a stabilizing effect introducing resonant and non-resonant interactions affecting the growth and real frequency.

Comparing these results with that of [14] in which they have studied the effect of inhomogeneous DC electric field instead of AC field, it is found that although the inhomogeneity in DC electric field has significant effect on the growth rate, but it remains effective only in localized region $k_\perp \rho_i < 3$. The increase in inhomogeneity increases the growth rate whereas increase of AC field frequency decreases the growth rate.

4. SUMMARY

Electrostatic ion-cyclotron parallel flow velocity shear instability has been studied in the presence of perpendicular AC electric field. The method of characteristic and kinetic approach has been adopted to evaluate the dispersion relation and growth rate. The effect of AC electric field, density gradient and velocity shear length has been studied in the region of ionosphere for long wavelength.

REFERENCES

1. Drummond, W. E. and M. N. Rosenbluth, "Anomalas diffusion a rising from microinstablities in a plasma," *Phys. Fluids*, Vol. 5, 1507, 1962.
2. Ganguli, G. and P. Bakshi, *Phys. Fluids*, Vol. 25, 1830, 1982.
3. Ganguli, G., P. Bakshi, and P. Palmadesso, *Phys. Fluids*, Vol. 26, 1808, 1983.
4. Ganguli, G., P. Bakshi, and P. Palmadeso, *Geophys. Rs.*, Vol. 89, 945, 1984.
5. Ganguli, G., P. Bakshi, and P. Palmadeso, *Phys. Fluids*, Vol. 27, 2039, 1984.
6. Chandrashekar, S. C., *Hydrodynamic and Hydro-magnetic Stability*, Ch. XI, Drover, New York, 1981.
7. Mikhailovskii, A. B., *Theory of Plasma Instabilities*, Vol. 1, Ch. 7, Constants Bereau, NewYork, 1974.
8. Maslowe, S. A., *Hydrodynamic Instabilities and Transition to Turbulance*, Ch. 7, Spinger Verlag, Berlin, 1985.
9. Waelbroeck, E. L. and F. L. Chen, *Phys. Fluids*, Vol. B3, 601, 1991.

10. Bhattacharjee, R., R. Iacono, J. L. Milovich, and C. Paranicas, *Phys. Fluids*, Vol. B1, 2207, 1989.
11. Biglari, H., P. H. Diamond, and P. W. Terry, *Phys. Fluids*, Vol. B2, 1, 1990.
12. Shaing, K. C. and E. C. Crume, Jr., *Phys. Rev. Lett.*, Vol. 63, 2369, 1989.
13. Groebner, R. J., K. H. Burrell, and R. P. Seray Darian, *Phys. Rev. Lett.*, Vol. 64, 3015, 1990.
14. Pandey, R. S., K. D. Misra, and A. K. Tripathi, "Generation of ion-cyclotron like wave by parallel flow velocity shear in the presence of inhomogeneous D.C. electric field in an anisotropic magnetoplasma," *Indian J. Radio Space Phys.*, Vol. 32, 75, 2003.
15. Mozer, F. S., C. W. Carlson, M. K. Hudson, R. B. Torbert, B. Parady, J. Yattean, and M. C. Kelly, *Phys. Rev. Lett.*, Vol. 38, 292, 1977.
16. Temerin, M., C. Cattell, R. Laysak, M. Hudson, R. B. Torbert, F. S. Mozer, R. D. Sharp, and P. M. Kintner, *J. Geophys. Res.*, Vol. 86, 11278, 1981.
17. Ganguli, G., Y. C. Lee, and J. Palmadesso, "Kinetic theory for electrostatic waves due to transverse velocity shear," *Phys. Fluids*, Vol. 31, 823, 1988.
18. Ganguli, G., Y. C. Lee, and P. J. Palmadesso, "Electrostatic ion-cyclotron instability caused by a non-unifrom electric field perpendicular to external magnetic field," *Phys. Fluids*, Vol. 28, 761, 1985.
19. Pandey, R. S., K. D. Misra, and A. K. Tripathi, "Kelvin-Helmholtz instability in an anisotropic magnetoplasma in the presence of inhomogeneous D.C. electric field parallel flow velocity shear," *Indian J. Radio Space Phys.*, Vol. 30, 113, 2001.
20. Pandey, R. S., R. P. Pandey, A. K. Srivastava, S. M. Karim, and Hariom, "The electromagnetic ion-cyclotron instability in the presence of a.c. electric field for Lorentzian kappa," *Progress In Electromagnetics Research M*, Vol. 1, 207, 2008.
21. Huba, J. D., "The Kelvin-Helmholtz instability in inhomogeneous plasma," *J. Geophys. Res.*, Vol. 86, 3653, 1981.